# Hierarchical structure description of spatiotemporal chaos

Jian Liu,[1] Zhen-Su She,[1,2,*] Hongyu Guo,[3] Liang Li,[3] and Qi Ouyang[3]
[1]*State Key Laboratory for Turbulence and Complex Systems and Department of Mechanics and Engineering Science, Peking University, Beijing 100871, People's Republic of China*
[2]*Department of Mathematics, UCLA, Los Angeles, California 90095, USA*
[3]*Department of Physics, Peking University, Beijing, 100871, People's Republic of China*
(Received 3 March 2004; revised manuscript received 24 May 2004; published 29 September 2004)

We develop a hierarchical structure (HS) analysis for quantitative description of statistical states of spatially extended systems. Examples discussed here include an experimental reaction-diffusion system with Belousov-Zhabotinsky kinetics, the two-dimensional complex Ginzburg-Landau equation, and the modified FitzHugh-Nagumon equation, which all show complex dynamics of spirals and defects. We demonstrate that the spatial-temporal fluctuation fields in the above-mentioned systems all display the HS similarity property originally proposed for the study of fully developed turbulence [Z.-S. She and E. Leveque, Phys. Rev. Lett. **72**, 336 (1994)]. The derived values of a HS parameter $\beta$ from experimental and numerical data in various physical regimes exhibit consistent trends and characterize the degree of turbulence in the systems near the transition, and the degree of heterogeneity of multiple disorders far from the transition. It is suggested that the HS analysis offers a useful quantitative description for the complex dynamics of two-dimensional spatiotemporal patterns.

DOI: 10.1103/PhysRevE.70.036215 PACS number(s): 05.45.−a, 82.40.Ck, 47.54.+r, 47.27.−i

## I. INTRODUCTION

Spatiotemporal chaos have been studied extensively in recent years with different levels of quantitative characterization [1]. It was discovered that for some spatially extended systems such as the Rayleigh-Bénard (RB) convection [2,3], an ordered state of straight or weakly curved rolls breaks down to a spatiotemporally chaotic state consisting of elementary spiral structures which appear and disappear in an irregular fashion. Spiral patterns driven far from equilibrium have also been studied in chemical reaction-diffusion systems such as Belousov-Zhabotinsky (BZ) reaction [4] and in biological systems such as cardiac muscle tissue [5]. While an individual spiral is considered as a self-organized topological defect, instabilities can lead to so-called defect-mediated turbulence [6] that is characterized by an exponential decay of correlations with length and time. There have been very fruitful efforts in the theoretical, experimental and numerical studies on the onset phase of the instability which results in the breaking down of spiral waves to the early transition to the disorder states (for a review on the complex Ginzburg-Landau (CGL) system, see Ref. [7]. The study of the transition via instabilities is important for problems such as the transition from spiral to spiral turbulence in heart tissue which plays an essential role in cardiac arrhythmia and fibrillation [5].

Another question often raised is what quantitative measures are useful when spatiotemporal patterns evolve, especially after spatiotemporal chaos are developed [7,8]. Attempt to identify defects and conduct statistical study of defects in defect-mediated turbulence has yielded some interesting results. In the discussion on the CGL system, it was argued [6] that the number of defects can be a convenient quantity to characterize spatiotemporal chaos. However, the relation between the finite-time dimension and the number of defects has not been fully established for systems of all sizes and of all duration intervals, and thus the method of separation has not appeared fully convincing [7]. In addition, when spatiotemporal pattern become chaotic, the identification of the basic structure (e.g., the defect) is not always possible, and its statistics become dubious. In general, spirals act more like waves than particles, but sometimes they may display spatially intermittent features. Note that, although the RB convection, the BZ reaction, and the CGL system all exhibit spiral wave behaviors and defect structures, the instabilities leading to complex spatiotemporal behaviors are of different nature. Moreover, local pattern structures may also appear in various forms of spiral, stripe, hexagon, or square. Nevertheless, transitions from ordered to disordered states exist in all these systems, and a common feature of these transitions is the generation of multiple scale fluctuations. Therefore, simple phenomenology independent of the details of the particular system is needed to reveal the essential feature of spatiotemporal chaos "buried in the wealth of available data" [8]. The present work propose such a simple phenomenology but with a quantitative measure.

There are several other quantitative measures proposed for characterizing disorder in pattern dynamics. Correlation length was directly estimated in experiments [9], and was also extracted from correlation functions [10] or from the width of so-called structure factors [11,12]. Hu *et al.* [13] proposed to use local wave numbers as an order parameter to characterize experimental RB patterns. Gunaratne *et al.* [14] suggested a disorder function to describe disordered patterns close to locally striped structures [15]. Egolf *et al.* [16] presented a simple algorithm for real-time quantitative analysis of local structure by computing the local wave number in disordered striped patterns. Newell and co-workers [17] used

*Email address: she@pku.edu.cn

 ©2004 The American Physical Society

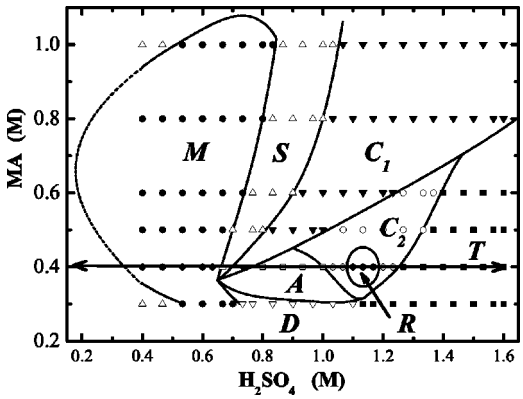


FIG. 1. The phase diagram of the BZ experiment reproduced from [18]. The concentrations $[\mathrm{MA}]^A$ and $[\mathrm{H_2SO_4}]^B$ are the control parameters. The solid lines indicate the onsets of different instabilities. The dashed lines are the extrapolation of the solid lines. The heavy line with arrows at $[\mathrm{MA}]^A = 0.4\mathrm{M}$ indicate the case studied here.

a wave-vector field determined by the wavelet transform to study the behavior of phase-diffusion equations in the presence of defects. All the methods mentioned above are effective to describe irregular patterns with "visually" distinct local structures such as local striped structure. When spatiotemporal chaos are overwhelmingly developed, however, local striped structures cannot be defined and these measures cannot be applied. This is the case for spiral turbulence in highly turbulent regimes of BZ experiments where either exact defect structures or characteristic wave numbers are difficult to obtain. The present study gives a different approach which may be applicable to much more disordered patterns.

The BZ reaction system is a particularly interesting system for the study of the spiral dynamics, where spirals can be supported in excitable or oscillatory media [1,4]. A recent experimental study [18] has systematically identified several regimes of spatial patterns resulted from two instabilities, a Doppler instability and a long wavelength instability. At various values of the chemical concentration in reservoir $A$ of malonic acid $[\mathrm{MA}]^A$ and in reservoir $B$ of sulfuric acid $[\mathrm{H_2SO_4}]^B$, the BZ reaction system displays a variety of patterns including (see Fig. 1 which is reproduced from Fig. 1 of Ref. [18]) the following: simply rotating spiral ($S$); meandering spiral ($M$); chemical turbulence due to the Doppler instability ($D$); abnormal chemical turbulence ($A$); renascent stable spiral ($R$); convectively unstable spiral ($C_1$ and $C_2$); and chemical turbulence due to the long wavelength instability ($T$). This rich set of spiral patterns is an ideal system for testing theoretical methods for characterizing spatiotemporal chaos.

We have proposed a hierarchical structure (HS) description of spatiotemporal chaos [18,19] based on an earlier HS model of She and Leveque for hydrodynamic turbulence [20,21]. The starting point of the analysis is to construct a multiscale probability density function (PDF) description for the fluctuation field of our interest, and then to develop a phenomenological model for the description of PDFs over the entire range of scales. This set of PDFs carries the probability information for fluctuations at different scales (large versus small) and at different intensities (tail events versus core events). The scale enters as a parameter when the fluctuation field is filtered for defining random variables, and the intensity is parametrized by the order of the moments calculated with the PDFs. Therefore, the dependence of the moments on the scale $\ell$ and on the order $p$ constitute a set of quantitative measures about the properties of the field.

The HS model gives a special compact description of this set of multiscale and multi-intensity properties. The basic idea in the HS model is that many statistically stationary multiscale fluctuation fields generated from nonlinear interactions between many degrees of freedom have a self-organized property expressible in terms of multifractal scaling whose multifractal dimension function can be understood in terms of a similarity relation between structures of increasing intensities of successive moment-order $p$ [20]. This new similarity relation was proposed for turbulence as a generalization of the Kolmogorov's complete scale similarity [21]. Later, it was discovered that the HS similarity is satisfied in a variety of nonlinear systems and other complex systems, such as the RB convection [22], the Couette-Taylor flow [23], flows in rapidly rotating annulus [24], the climate variations [25], the variation of nucleotide density along DNA sequences [26], the diffusion-limited aggregates [27], a fluctuating luminosity field of natural images [28] and several others [29]. More interestingly, the previous studies show that the derived HS parameters are closely related to global property of the turbulent system. For example, in Couette-Taylor flow, one HS parameter gives a signature of the breaking down of the Taylor vortex [23]. It is thus hoped that the HS analysis would shed light on the properties of a fluctuation field displaying spatiotemporal chaos.

In [18,19], the HS analysis is briefly applied to describe the spiral turbulence in the BZ experiment and in the numerical solutions of the two-dimensional CGL equation. It was shown that the HS similarity is accurately verified for various experimental and numerical two-dimensional fluctuation fields which include both the ordered spirals and spatiotemporal chaos. In the study of the BZ experiment, it is discovered that the measured HS parameter $\beta$ shows a transition when the system undergoes a transition from one kind of spiral turbulence state to another (e.g., from the state $D$ to the state $T$ in Fig. 1). Those preliminary findings have inspired the present detailed study of the nature of $\beta$ while a more complex sequence of transitions are analyzed and more numerical models are considered.

Specifically, we will examine more experimental data with transitions between complex states. In Fig. 1, at $[\mathrm{MA}]^A = 0.4$, the patterns vary through $M$, $S$, $C_1$, $A$, $C_2$, $R$, and $T$. During the transition, the amount of order (e.g., spiral structures), the degree of heterogeneity (with the mixing of ordered and disordered structures) and intermittency vary with parameters. We will show that $\beta$ characterizes such transitions near and far from the threshold in the experimental BZ system. We supplement this with a further detailed study of the spiral dynamics in the CGL equation [7] and in a two-component model equation called modified FitzHugh-Nagumo (MFN) model [30,31] which has a number of ap-

plications in biological systems. In all cases, we focus on the validity of the HS description and the explanation of the dynamics in terms of the degree of heterogeneity and of intermittency that the value of $\beta$ indicates. We believe that the relationship between the values of $\beta$ and the dynamics of spatiotemporal patterns is valuable.

The paper is organized as follows. In Sec. II, we present briefly the HS model with special emphasis on the method of the HS similarity test ($\beta$-test) and the explanation of the meaning of $\beta$. Section III is devoted to the analysis of a sequence of complex transitions in the experimental BZ system. In Sec. IV, we carry out a detailed study of the transition of the spiral dynamics in the CGL equation and the MFN equation. Section V offers a summary and some additional discussion.

## II. THE HS DESCRIPTION

The HS model has been originally proposed by She and Leveque to describe inertial-range multiscale fluctuations in a turbulent fluid. The key concept in the model is a hierarchy of moment ratios. Let $\varepsilon_\ell$ denote a certain characteristic variable characterizing fluctuations of the physical system at the length scale $\ell$. Define the $p$th-order moments $S_p(\ell)=\langle|\varepsilon_\ell|^p\rangle$. The HS model introduce a hierarchy of functions:

$$F_p(\ell)=\frac{S_{p+1}(\ell)}{S_p(\ell)}, \tag{1}$$

each of which has the physical dimension of $\varepsilon_\ell$ and hence describes a certain amplitude of the fluctuations. The function $F_p(\ell)$ depends on the probability density functions (PDFs) of $\varepsilon_\ell$. For a typical set of PDFs of a turbulent field and of a spatiotemporal field as we study in this work, the function $F_p(\ell)$ increases with $p$. In other words, $F_p(\ell)$ at higher $p$ is associated with higher intensity fluctuation structures. We refer $F_p(\ell)$ to as the $p$th-order HS function.

An intuitive idea in the HS model is that in a self-organized dynamical steady state, there is a similarity in the dependence of $F_p(\ell)$ on $\ell$ for different $p$'s ($0\leqslant p\leqslant\infty$). In the case of scaling dependence on $\ell$, the simplest similarity is that all $F_p(\ell)$ have the same scaling. This corresponds to the Kolmogorov 1941 (K41) theory of turbulence in which the large and small scale statistics are completely self-similar. For example, when $\varepsilon_\ell$ represents the locally averaged dissipation, then the K41 theory predicts that $F_p(\ell)\sim F_0(\ell)=\langle\varepsilon_\ell\rangle\sim\ell^0$ (the mean dissipation is equal to the average energy flux that is constant independent of the scale). This complete self-similarity law has been demonstrated invalid in experiments and numerical simulations during the past decade, and the dissipation fluctuations have anomalous scalings in $\ell$. This is the so-called intermittency effect [33].

She and Leveque [20] postulate that the most intense structure $F_\infty(\ell)=\lim_{p\to\infty}F_p(\ell)$ plays a special role, and all other fluctuation structures of finite $p$ obey a hierarchical similarity law, namely

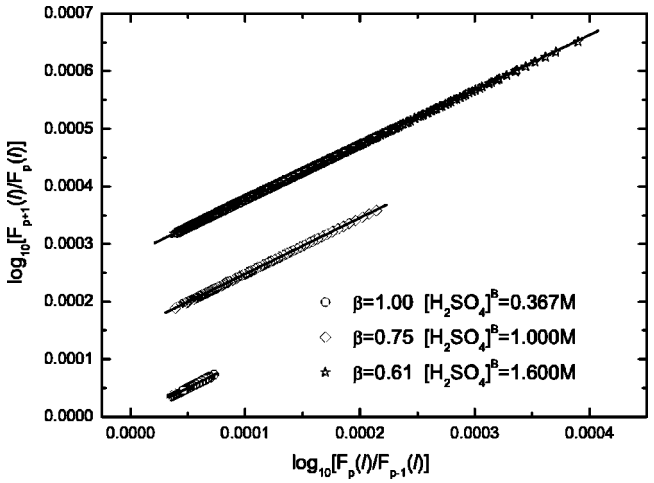


FIG. 2. The HS similarity test for three patterns from the experimental BZ system: $[H_2SO_4]^B=0.367$M, 1.0M, and 1.6M. The other control parameter is fixed at $[MA]^A=0.4$M. A straight line indicates the validity of the HS similarity. The slope $\beta$ is estimated by a least square fitting. For clarity, the second and third set of data points are displaced vertically up by a suitable amount.

$$\frac{F_{p+1}(\ell)}{F_\infty(\ell)}=A_p\left(\frac{F_p(\ell)}{F_\infty(\ell)}\right)^\beta, \tag{2}$$

where $0\leqslant\beta\leqslant1$, $A_p$ are independent of $\ell$. The term $F_\infty(\ell)$ can be eliminated by considering the ratio

$$\frac{F_{p+1}(\ell)}{F_p(\ell)}=\frac{A_p}{A_{p-1}}\left(\frac{F_p(\ell)}{F_{p-1}(\ell)}\right)^\beta. \tag{3}$$

Both sides of Eq. (3) can be computed from the empirical PDFs (or histograms) of $\varepsilon_\ell$ calculated from an experimental or numerical fluctuation field. The linearity in the log-log plot of Eq. (3) can be a direct test of the validity of Eq. (2). This will be refer to as the HS similarity test, or the $\beta$ test [23,34]. Figure 2 shows the result of applying the $\beta$ test to the data of experimental BZ reaction (for details, see below). The linear relation is obviously verified, and the slope $\beta$ can be accurately estimated.

The meaning of the parameter $\beta$ can be readily obtained from the definition Eq. (2) [21,23]. It describes a kind of discrepancy between $F_{p+1}$ and $F_p$. When $\beta$ approaches 1, high $p$ (intense) structures and low $p$ (weak) structures are alike. This may be realized at either extremely ordered states or completely homogeneous disordered states. In the former, the structures of various intensities are strongly correlated. Below, we will report observations of this $\beta$ for ordered spiral states. The latter situation corresponds to the hypothetical field postulated by the K41 theory with complete self-similarity; unfortunately, it has not yet been observed in real physical system. Another extreme case is the limit $\beta\to0$. This is the case in which $F_\infty(\ell)$ stands out as the only kind of singular structure which is responsible for the physical process. A mathematical model displaying the dynamics of one-dimensional shocks, the so-called Burgers equation, exhibits behavior close to this description, where only shocks at iso-

lated points are responsible for the energy dissipation and all statistical moments are determined by the discontinuities across the shocks.

The study of hydrodynamic turbulence reveals that in many realistic turbulent systems, $0<\beta<1$, namely the most intense fluctuations do not completely dominate and the fluctuation structures of various intensities are not completely alike. The fluctuation structures of various intensities are all responsible for the physical process, but they are related by the hierarchical similarity law Eq. (2) which we believe is a form of the self-organization of the system.

The results reported below on the experimental BZ system and numerical spiral dynamics demonstrate that when the hierarchical similarity holds, the parameter $\beta$ gives a quantitative description of the degree of order or disorder and of homogeneity or heterogeneity. For $\beta$ close to one, the system appears to be orderly homogeneous and orderly self-organized; for moderately smaller $\beta$ the system contains a mixture of order and disorder and appears to be heterogeneous. The smallest $\beta$ indicates the appearance of overwhelmingly disordered and intermittent state with fully developed spatiotemporal chaos. The details of these findings are reported below.

### III. ANALYSIS OF EXPERIMENTAL BZ SYSTEM

The experimental BZ system analyzed here has been described in detail in Ref. [18]. An extensive phase diagram (see Fig. 1) is established in the two-dimensional plane formed by the concentration $[H_2SO_4]^B$ versus $[MA]^A$, in which various pattern dynamical states are identified based (essentially) on visual inspection of experimental images or luminosity fields. The HS analysis is performed on the total variation field, $G(x,y)$, rather than directly on the luminosity (image) field $f(x,y)$: which is proportional to the chemical concentration:

$$G(x,y)=\left[\left(\frac{\partial f}{\partial x}\right)^2+\left(\frac{\partial f}{\partial y}\right)^2\right]^{1/2}. \tag{4}$$

Then, we construct a set of multiscale variables to be the coarse-grained local variation field, $\varepsilon_\ell$, similar to the locally averaged energy dissipation in turbulence, which is defined as below:

$$\varepsilon_\ell=\frac{1}{\ell^2}\int_x^{x+\ell}\int_y^{y+\ell} G(f(x',y'))dx'dy'. \tag{5}$$

We examine the statistical properties by calculating the moments of $\varepsilon_\ell$ as $\ell$ varying for increasing control parameter $[H_2SO_4]^B$. The moments $S_p(\ell)=\langle|\varepsilon_\ell|^p\rangle$ are calculated by a space average of $256\times256$ pixels and by a time average over a number of images collected at different times. Furthermore, the HS functions $F_p(\ell)$ are calculated and the ratio across successive orders are evaluated and plotted, as in Fig. 2. It is readily seen that the hierarchical similarity is satisfied and the HS parameter $\beta$ can be obtained (by a least square fitting) with a good accuracy. Technically speaking, this completes the HS analysis of a fluctuation field at a given control parameter.

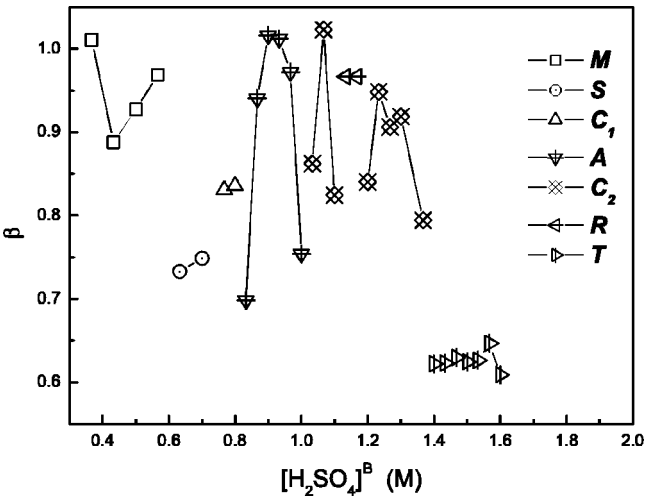


FIG. 3. The HS similarity parameter $\beta$ as a function of the control parameter $[H_2SO_4]^B$ with fixed $[MA]^A=0.4$M. Symbols indicate the pattern regimes as found experimentally (see the text for detailed explanation).

Detailed examinations of the values of $\beta$ at various control parameters constitute a further step in the analysis. The variation of $\beta$ for all patterns observed in the experiment at each parameter value of $[H_2SO_4]^B$ is recorded in Fig. 3. The values of $\beta$ seem to exhibit strong fluctuations, and it seems that there is no simple correspondence between the value of $\beta$ and the regime. More careful inspection reveals, however, that $\beta$ describes the property of the pattern as expected from the theoretical consideration above. We attempt to itemize our observations as follows:

(a) For the ordered patterns, the values of $\beta$ measured are close to one. In Fig. 4(a), we plot a typical experimental image of the ordered spiral state ($M$) with $\beta=1$. Theoretically speaking, $\beta=1$ implies that low and high intensity structures are alike, which happens with an ordered pattern. Note that some values of measured $\beta$ are not close to one for ordered spiral states (e.g., the two $S$ states for which $\beta\approx0.75$ in Fig. 3). One possible explanation for the exception of the two $S$ states with low $\beta$ is the existence of experimental noise (e.g., dark spots in the experimental images) that introduces artificially *sharp* structures in the field. Our studies show that such "intrusion" of sharp objects lead to a decrease of $\beta$.

(b) Near the transition between one regime and another, we observe a depletion of the value of $\beta$ compared to that measured for the states far from the transition (see Fig. 3). We plot a typical experimental image near the transition between $C_1$ and $A$ in Fig. 4(b) with $\beta=0.7$. Theoretically speaking, a lower value of $\beta$ indicates a higher intermittency of the spatial patterns. Figure 4(b) indeed shows a mixture of ordered spirals and disordered irregular spiral elements, which displays clearly a strong heterogeneity. We conclude that one kind of intermittency in spatially extended systems is related to heterogeneous composition of patterns of different origins. In addition, we conclude that a sharp variation of $\beta$ usually indicates a transition of regimes. This finding is interesting for defining statistical regimes. We believe that this is the most interesting finding of this work.

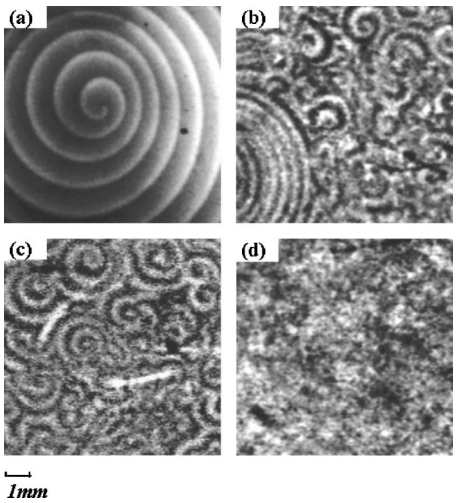


FIG. 4. Optical images of typical experimental states obtained with different $[H_2SO_4]^B$: (a) an ordered state with 0.367M, $\beta=1.0$; (b) a heterogeneous disordered state (coexistence of spiral waves and spatiotemporal chaos) with 0.833M, $\beta=0.7$; (c) an abnormal turbulent state with 0.867M, $\beta=0.94$; (d) a homogeneous intermittent disordered state with 1.4M, $\beta=0.62$. The parameter $[MA]^A$ are fixed at 0.4M. The region shown is $8.5\times8.5$ mm$^2$ out of a disk of 20 mm$^2$ in diameter.

(c) In fully developed spatiotemporally chaotic states, the spatial patterns develop small-scale intermittent structures and yield even smaller values of $\beta$ ($<0.65$). In Fig. 4(d), we show an experimental image for the chemical turbulent state $T$ with $\beta=0.62$. It is clear that very small characteristic scales are developed in the patterns which signify large fluctuations in the total variation field (because of the spatial derivatives). This enhanced intermittency appears to be stronger than noted in item (b).

(d) There are also other disordered states (e.g., $A$ and $C_2$) for which $\beta$ is close to one. Close inspection shows that these disordered states all encompass large-scale irregular spiral elements, as shown in Fig. 4(c) where $\beta=0.94$. These large-scale patterns are quite homogeneous and spatially ordered, which may yield a large value of $\beta$. Note that the HS analysis conducted in this paper is a spatially multiscaling analysis which describes only the property of instantaneous spatial patterns. Our conclusion is that the states in the regimes $A$ and $C_2$ involve only spatially ordered patterns with actively temporal dynamics. They are distinguished from the other chaotic states like $T$ and $D$.

The above analysis helps to understand the nature of the parameter $\beta$ in the HS analysis of spatiotemporal chaos, and confirms our previous finding that $\beta$'s variation reveals a transition between two different spatiotemporally chaotic states. The spiral turbulence state due to the Doppler instability has a characteristic scale larger than that in the spiral turbulence state due to the long wavelength instability. Both states are homogeneously chaotic, but the later contains more intermittent small-scale structures. The HS analysis is suitable to capture such difference.

## IV. ANALYSIS OF NUMERICAL SPIRAL TURBULENCE

We now turn to the analysis of numerically simulated two-dimensional spatiotemporal dynamics. First, in numerical calculations, the interaction mechanism responsible for the generation of spatial patterns is under good control, so that spatial patterns are free of noises and perturbations that are inevitable in experiments. For example, optical artifacts in the experimental images pose great challenge to the HS analysis (in the calculation of the total variation field) and thus compromise the clarity of the finding. Secondly, the experimental states analyzed above are all asymptotical states. We are also interested in the characterization of transient states. In other words, we are interested in testing whether the HS description can characterize the property of a spatial pattern which undergoes actively dynamical evolution. Numerical simulations provide a detailed sequence of patterns under dynamic evolution. Finally, the present analysis of numerically simulated field may inspire further studies of a variety of two-dimensional partial differential equations of pattern dynamics, e.g., the Navier-Stokes equation for the vortex dynamics. Such empirical studies are important to the finding of right order parameters of chaotic pattern dynamics.

We will study two model equations for the pattern dynamics leading to spatiotemporal chaos. The first equation is the two-dimensional CGL equation:

$$\frac{\partial A}{\partial t} = A + (1 + ic_1)\Delta A - (1 + ic_3)|A|^2 A, \tag{6}$$

where $A(\boldsymbol{r},t)$ is a complex function of time ($t$) and space ($\boldsymbol{r}$), the real parameters $c_1$ and $c_3$ are coefficients characterizing linear and nonlinear dispersion, respectively. Although the CGL equation is a normal form relevant only near the threshold of a supercritical Hopf bifurcation, it has become a popular model to study spatiotemporal chaos where oscillations and waves are present [1,7]. Indeed, our simulation gives rise to both simple spiral waves and chaotic states which encompass many disordered spatiotemporal oscillations.

The numerical study of Eq. (6) is performed using an Euler algorithm with no-flux boundary condition on a $256\times256$ square lattice and a time step of $\Delta t=0.03$. The initial conditions are chosen to be a simple spiral wave which is the stable solution when $c_1=-1.40$ and $c_3=0.50$. We then keep $c_1$ fixed and increase $c_3$ to explore possibly alternative patterns. We choose to analyze the fluctuation properties of the real part $f(x,y)$ of the complex field $A(x,y)=f(x,y)+ig(x,y)$. The details of the computation and the transition leading to spatiotemporal chaos can be found in Ref. [19], where we have established the fact that the $\beta$ test is satisfied in both ordered spiral states and spatiotemporal chaos states. In the present work, we report the result of a systematic HS analysis of a sequence of patterns with varying parameters.

Four snapshots of the field $f(x,y)$ are shown in Fig. 5, which contribute to a so-called far-field breaking-up process. As $c_3$ increases, the convective instability occurs and the spiral wave breaks up far from the tip. In a range of intermediate values of $c_3$, the spiral wave coexists with spatiotemporal chaos surrounding it. Finally, at high values of $C_3$, the spiral wave totally breaks up and spatiotemporal chaos dominate the whole box ($c_3>0.76$).

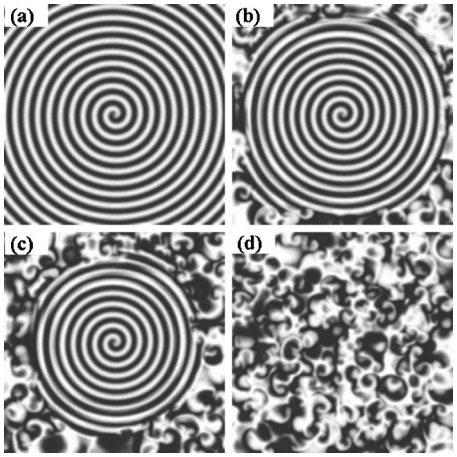


FIG. 5. Snapshots of the field $f(x,y)$ from the CGL equation at four different parameter values of $c_3$. (a) Stable spiral, $c_3=0.6$; (b) coexistence of spiral and spatiotemporal chaos, $c_3=0.74$; (c) coexistence of spiral and spatiotemporal chaos, $c_3=0.75$; (d) fully spatiotemporal chaos, $c_3=0.8$.

The HS analysis of the solutions of the CGL equation begins with the construction of the total variation field. Let $G(x,y)$ be defined as in Eq. (4) with the field $f(x,y)$. The coarse-grained local variation field, $\varepsilon_\ell$, is defined as in Eq. (5). The same procedure of the $\beta$ test as explained in the previous section is now applied to the data $\varepsilon_\ell$. As shown in Fig. 6, good linearity and hence the HS similarity are obtained for all the states of both ordered spirals and irregular spiral turbulence, consistent with the result reported previously [19] and similar to that in Fig. 2. Note again that the values of $\beta$ are close to one for ordered spiral states, but significantly below one ($<0.9$) when spatiotemporal chaos are developed.

The variation of $\beta$ as a function of $c_3$ is shown in Fig. 7. All ordered spiral states have $\beta$ very close to one, and the

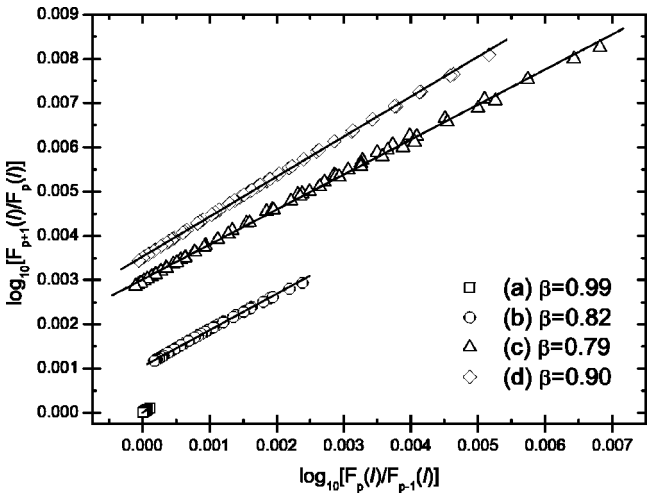


FIG. 6. The HS similarity test for the four patterns in Fig. 5 of the CGL equation. A straight line indicates the validity of the HS similarity. The slope $\beta$ is estimated by a least square fitting. For clarity, the second, the third, and the fourth set of data points are displaced vertically up by a suitable amount.

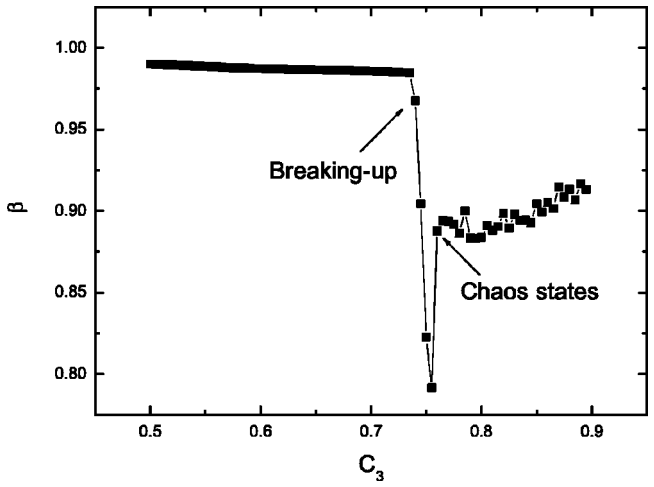


FIG. 7. The HS similarity parameter $\beta$ as a function of the control parameter $c_3$ in the CGL equation. Note a clear transition from an ordered state to a spatiotemporally chaotic state.

appearance of the irregular patterns surrounding the central spiral leads to a smaller $\beta$. It is interesting to note that the final chaotic states at high $c_3$ have a $\beta\approx0.9$ which is bigger than that of the transitional states with a mixture of ordered spirals and chaos. This fact is consistent with the previous finding in the analysis of the experimental BZ system that the mixed states near the transition are more heterogeneous and tend to have smaller $\beta$.

Another interesting aspect of the numerical CGL dynamics is the possibility to follow closely a spontaneous generation of spatial disorder from an ordered state. A sequence of dynamically evolving patterns are shown in Fig. 8, where the spiral core breaks up without meandering and then subsequently develops to a complete spatiotemporal chaotic pattern. This fast breaking-up process is phenomenologically similar to that of the Doppler instability [4,32], but with the spiral center fixed. The details of the explanation for this process can be found in Ref. [19]. Here, we show four typical snapshots of the spatial pattern at successive times with fixed control parameter $c_1=-1.40$ and $c_3=0.8$.

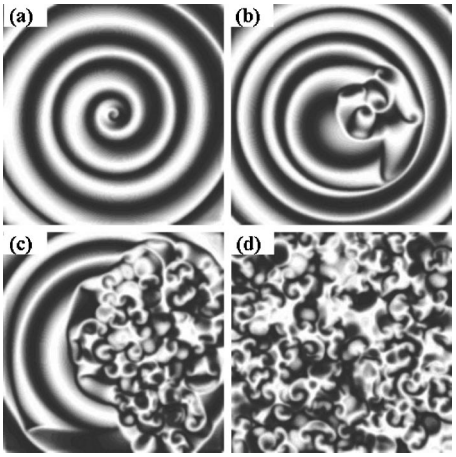


FIG. 8. A sequence of evolving fields $f(x,y)$ from the CGL equation at different times. (a) $t=390$; (b) $t=500$; (c) $t=550$; (d) $t=770$.

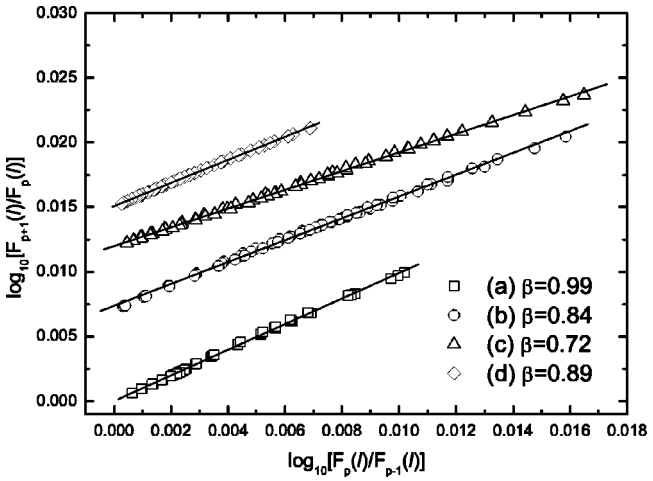


FIG. 9. The HS similarity test for the four patterns in Fig. 8 of the CGL equation. A straight line indicates the validity of the HS similarity. The slope $\beta$ is estimated by a least square fitting. For clarity, the second, the third, and the fourth set of data points are displaced vertically up by a suitable amount.

Figure 9 reports the result of the $\beta$ test for the corresponding four pattern states in Fig. 8. Good HS similarity property is found for all pattern states, including the single spiral ($\beta \approx 1$), the intermediate state with generated defects ($\beta < 0.9$) and the full developed turbulent state ($\beta \approx 0.9$). Figure 10 shows the variation of $\beta$ as a function of time during the core breaking up. The parameter $\beta$ begins with a value close to one and undergoes a transition when disorder is developed. At $t \approx 550$, $\beta$ reaches the minimum value when disorder is mixed with order. Later, $\beta$ increases again because of the homogeneity of the disorder. These facts are consistent with the observations reported earlier. Once more, the HS parameter $\beta$ acts as an order parameter to the description of the evolution of the CGL system from the ordered spiral to the disordered spatiotemporal chaos.

The second model equation we have studied is a simple activator-inhibitor model: the two-dimensional MFN model

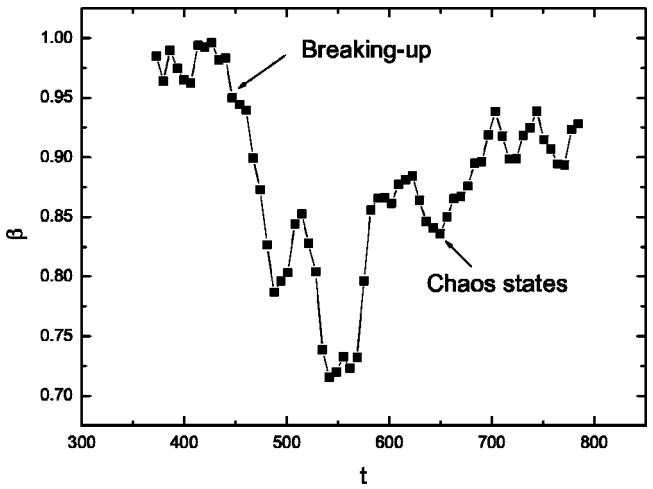


FIG. 10. The HS similarity parameter $\beta$ as a function of time for a sequence of evolving patterns in the CGL equation. Note that $\beta$ acts as an order parameter revealing the transition from an ordered state to a spatiotemporally chaotic state.

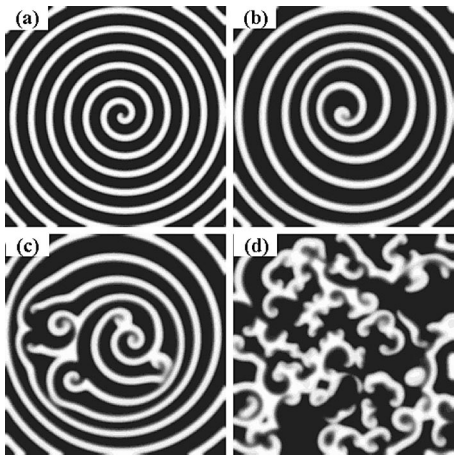


FIG. 11. Snapshots of the field of the fast activator $u$ in the MFN equation. (a) Simple spiral, $\sigma = 0.0525$; (b) meandering spiral, $\sigma = 0.07$; (c) outbreak of breaking-up spiral, $\sigma = 0.0725$; (d) spatiotemporal chaos, $\sigma = 0.075$. Other parameters are $a = 0.84$, $b = 0.07$.

[30,31]. While the CGL equation describes an oscillatory dynamics (with two components representing the real and imaginary parts of a complex variable field), the MFN model is a two-component model of an excitable system in which a fast activator ($u$) and a slow inhibitor ($v$) are in interaction:

$$u_t = -\frac{1}{\sigma} u(u-1)\left[u - \frac{v+b}{a}\right] + \Delta u, \tag{7a}$$

$$v_t = f(u) - v, \tag{7b}$$

$$f(u) = \begin{cases} 0, & 0 \leqslant u < \frac{1}{3}, \\ 1 - 6.75u(u-1)^2, & \frac{1}{3} \leqslant u \leqslant 1, \\ 1, & u > 1, \end{cases} \tag{7c}$$

where the form of $f(u)$ describes an inhibitor production only above a threshold value of $u$, and the value of $\sigma$ related to the time scales of both activator ($u$) and inhibitor ($v$) measures the degree of excitability. A nice feature of the MFN model is that the degree of the excitability of the medium can be continuously modified by varying the parameters. It is known [30] that fast activator dynamics ($0 < \sigma \ll 1$) and suitable choice for other parameters ($a < 1$, $b > 0$) lead to excitability. When one fixes the parameters $a$ and $b$ and gradually increases $\sigma$, the excited spiral waves will lose its stability, begin to meander, then break up at the tip, and spread chaotic spiral elements outward. Finally, the system develops a state of spatiotemporal chaos. This scenario is illustrated in Fig. 11, which contains a sequence of images of gray-scale picture of the activator $u$ obtained at various times of a dynamic evolution.

The numerical calculation of Eq. (7) reported above uses an Euler algorithm with noflux boundary condition on a $256 \times 256$ square lattice. The data presented in Fig. 11 are obtained with fixed parameters $a = 0.84$ and $b = 0.07$, but with several different values of $\sigma$. The simulation starts with a simple spiral initial condition that is the stable solution of the system at smaller values of $\sigma$ (e.g., $\sigma = 0.50$). At $\sigma = 0.725$, a

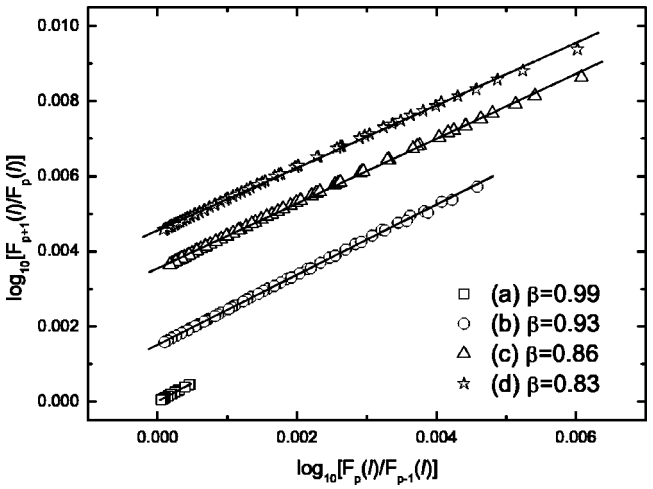


FIG. 12. The HS similarity test for the four pattern states in Fig. 11 of the MFN equation. A straight line indicates the validity of the HS similarity. The slope $\beta$ is estimated by a least square fitting. For clarity, the second, the third, and the fourth set of data points are displaced vertically up by a suitable amount.

transition from the simple spiral to spatiotemporal chaos as described earlier is fully realized.

To carry out the HS analysis, the total variation field $G(x,y)$ for the MFN model is calculated from the fast activator field $u(x,y)$ as in Eq. (4). The coarse-grained local variation field, $\varepsilon_\ell$, is defined as in Eq. (5). We have applied the $\beta$ test for the moments of $\varepsilon_\ell$, and the result is shown in Fig. 12. Clearly, the hierarchical similarity is verified for all values of $\sigma$ and the values of $\beta$ are derived accurately in all cases. The variation of $\beta$ as a function of $\sigma$ is presented in Fig. 13. The correspondence between the degrees of orders or disorder and the values of $\beta$ is quite clear, as shown in the study of the CGL equation. As the parameter $\sigma$ increases, the pattern gradually loses the correlation and $\beta$ decreases. Detailed examination shows that the tip of the spiral wave begins to meander at $\sigma=0.625$, and completely breaks up at $\sigma=0.725$. The breakup of the tip of the spiral marks the transition from $\beta\approx 1$ to $\beta\approx 0.8$. The later state corresponds to a fully developed spatiotemporal chaos.

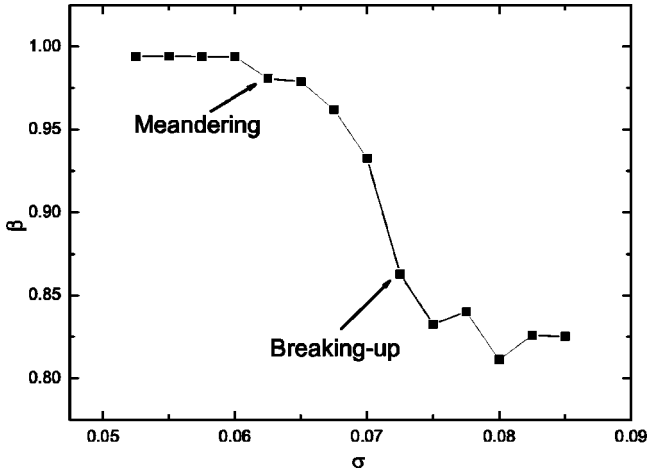


FIG. 13. The HS similarity parameter $\beta$ as a function of the control parameter $\sigma$ in the MFN equation. Note a clear transition from an ordered state to a spatiotemporal chaotic state.

The above numerical studies reveal that the CGL and MFN model equations have less complicated patterns than those in the experimental BZ system. This significantly reduces the complexity of the matter, and renders the HS description of the dynamics easy to interpret. It is worth noting that the numerical data are free from complicated disturbance so that the values of $\beta$ show a consistent trend of variation with less fluctuations, compared to the results of Fig. 3. We therefore find the convincing evidence that the HS parameter $\beta$ is like an order parameter that describes the transition from an ordered spiral state to a homogeneous disordered spiral turbulence.

## V. SUMMARY AND DISCUSSION

One of the most interesting problems in the study of the pattern dynamics is to find a quantitative measure that describes the global property of the pattern in both ordered states and turbulent states. When spatiotemporal chaos prevail and the effective number of degrees of freedom is large, many familiar quantities in the study of dynamical systems and chaos become hard to evaluate. On the other hands, traditional statistical measures such as correlation length also become ineffective when the pattern presents intermittent features. A new sound phenomenology is needed to capture subtle correlations across multiple scales and multiple fluctuation intensities.

We present here a sound phenomenology, the HS model, that gives a concise description of a spatiotemporal field by its multifractal scaling properties in terms of the HS parameter $\beta$. In this work, we present detailed evidence, based on analyzing experimental BZ system and numerical CGL and MFN model, that the HS similarity holds for all the fields (ordered or disordered) and the derived parameter $\beta$ describes the strength of the correlation across scales and across intensities. For $\beta$ close to one, the pattern is strongly correlated or ordered; a smaller $\beta$ implies a higher degree of heterogeneity and a mixture of order and disorder; the smallest $\beta$ is related to the intermittency associated with fully developed spatiotemporal chaos. In particular, our analysis has identified two different disordered states in the BZ experiment: the heterogeneous disordered state with a mixture of spirals and irregular spiral elements and the disordered and intermittent state of fully developed spatiotemporal chaos. In those cases, $\beta$ provides a useful characterization of the patterns in transition.

Based on the above results, we speculate that the HS similarity is an emergent property of self-organized complex nonlinear multiscale systems in general. This property, like the maximum entropy property of the thermal equilibrium state, may be difficult to be derived directly from the first principle (such as the Navier-Stokes equation for fluids or the Newtonian mechanical law for gases). It is thus important to conduct more empirical studies for proving or disproving the above conjecture, or for assessing its limit of validity.

For the quantitative analysis of spatiotemporal chaos, we believe that it is important to go beyond the simple statistics

for defects, wave numbers, or other local pattern properties, since often they are hard to be determined when spatial patterns become overwhelmingly irregular. The HS analysis is a global method that takes into account the properties of the whole field, but emphasizes at the same time subtle correlations and similarities among structures at multiple scales and multiple intensities. While the previous work [18,19] establishes the validity of the HS model for describing both experimental and numerical spiral patterns, the present work gives detailed evidence that the HS order parameter ($\beta$) characterizes the degree of heterogeneity and intermittency of spatial patterns and is particularly suitable for describing the evolution of patterns from ordered states to fully developed spatiotemporally chaotic states. This is demonstrated in the BZ, CGL and MFN systems. Our approach may be easily extended to describe other complex pattern-formation systems with different unit "cells" than spirals, such as strips, hexagons, squares, triangles, etc., and this is one of the advantages of the HS analysis.

To make a concise description for all these statistical properties, a phenomenology is required. The HS analysis is one of the plausible phenomenological proposals that rest on empirical observations ($\beta$ test). The fact that the HS similarity is found to be valid for a wide class of nonlinear processes indicates the possible universal mechanism or principle behind these processes. It is not yet clear how this universality should be expressed (e.g., in terms of a variational principle like the maximum entropy and minimum entropy production), but we believe that it deserves special attention in future studies.

## ACKNOWLEDGMENTS

We have benefited from the research environment at the LTCS of Peking University. The computation work is helped by the Turbulence Simulation Center of the LTCS. We acknowledge the support by the National Natural Science Foundation of China, No. 10225210, and by the State Key Project for Basic Research No. 2000077305.

[1] M. C. Cross and P. C. Hohenberg, Rev. Mod. Phys. **65**, 851 (1993).
[2] S. W. Morris, E. Bodenschatz, D. S. Cannell, and G. Ahlers, Phys. Rev. Lett. **71**, 2026 (1993).
[3] M. Assenheimer and V. Steinberg, Nature (London) **367**, 345 (1994).
[4] L. Q. Zhou and Q. Ouyang, J. Phys. Chem. A **105**, 112 (2001).
[5] A. T. Winfree, Science **266**, 1003 (1994); F. X. Witkowski, L. J. Leon, P. A. Penkoske, W. R. Giles, M. L. Spanol, W. L. Ditto, and A. T. Winfree, Nature (London) **392**, 78 (1998).
[6] P. Coullet, L. Gil, and J. Lega, Phys. Rev. Lett. **62**, 1619 (1989).
[7] I. S. Aranson and L. Kramer, Rev. Mod. Phys. **74**, 99 (2002).
[8] M. C. Cross and P. C. Hohenberg, Science **263**, 1569 (1994).
[9] Q. Ouyang and H. L. Swinney, Chaos **1**, 411 (1991).
[10] M. C. Cross and D. I. Meiron, Phys. Rev. Lett. **75**, 2152 (1995).
[11] K. R. Elder, J. D. Gunton, and N. Goldenfeld, Phys. Rev. E **56**, 1631 (1997); T. Galla and E. Moro, *ibid.* **67**, 035101 (2003).
[12] Structure factors were first used as a measure of the structure of local RB patterns in Ref. [2]. Detail comments on the usage of structure factor can be found in Ref. [13]. This measure has also been used to measure the growth of pattern domains, as in Ref. [10] and L. Purvis and M. Dennin, Phys. Rev. Lett. **86**, 5898 (2001).
[13] Y. Hu, R. Ecke, and G. Ahlers, Phys. Rev. E **51**, 3263 (1995); Phys. Rev. Lett. **74**, 391 (1995); Phys. Rev. E **55**, 6928 (1997).
[14] G. H. Gunaratne, R. E. Jones, Q. Ouyang, and H. L. Swinney, Phys. Rev. Lett. **75**, 3281 (1995); G. H. Gunaratne, D. K. Hoffman, and D. J. Kouri, Phys. Rev. E **57**, 5146 (1998); G. H. Gunaratne, A. Ratnaweera, and K. Tennekone, *ibid.* **59**, 5058 (1999).
[15] The disorder function calculates the local curvature of contour lines and local characteristic wavenumber for patterns of local stripped structures. For more complicated patterns, the calculation of the disorder function is difficult. Detail comments can be seen in Ref. [14].
[16] D. A. Egolf, I. V. Melnikov, and E. Bodenschatz, Phys. Rev. Lett. **80**, 3228 (1998).
[17] C. Bowman and A. C. Newell, Rev. Mod. Phys. **70**, 289 (1998).
[18] H. Y. Guo, L. Li, Q. Ouyang, J. Liu, and Z.-S. She, J. Chem. Phys. **118**, 5038 (2003).
[19] J. Liu, Z.-S. She, Q. Ouyang, and X. T. He, Int. J. Mod. Phys. B **17**, 4139 (2003).
[20] Z.-S. She and E. Leveque, Phys. Rev. Lett. **72**, 336 (1994); Z.-S. She and E. C. Waymire, *ibid.* **74**, 262 (1995).
[21] Z.-S. She, Prog. Theor. Phys. Suppl. **130**, 87 (1998).
[22] E. S. C. Ching, Acta Mech. Sin. **19**, 385 (2003); E. S. C. Ching, C. K. Leung, X. L. Qiu, and P. Tong, Phys. Rev. E **68**, 026307, (2003); E. S. C. Ching and C. Y. Kwok, *ibid.* **62**, R7587 (2000).
[23] Z.-S. She, K. Ren, G. S. Lewis, and H. L. Swinney, Phys. Rev. E **64**, 016308 (2001).
[24] C. Baroud, B. Plapp, H. Swinney, and Z.-S. She, Phys. Fluids **15**, 2091 (2003).
[25] Z.-S. She, Z. T. Fu, J. Chen, S. Liang, and S. D. Liu, Prog. Nat. Sci. **12**, 747 (2002).
[26] J. Wang, Q. D. Zhang, K. Ren, and Z.-S. She, Chin. Sci. Bull. **46**, 1988 (2001).
[27] D. Queiros-Conde, Phys. Rev. Lett. **78**, 4426 (1997).
[28] A. Turiel, G. Mato, N. Parga, and J.-P. Nadal, Phys. Rev. Lett. **80**, 1098 (1998).
[29] G. Ruiz Chavarria, C. Baudet, and S. Ciliberto, Physica D **99**, 369 (1996); E. Leveque, G. Ruiz-Chavarria, C. Baudet, and S. Ciliberto, Phys. Fluids **11**, 1869 (1999).

[30] M. Bär and M. Eiswirth, Phys. Rev. E **48**, R1635 (1993).
[31] D. Barkley, M. Kness, and L. S. Tuckerman, Phys. Rev. A **42**, 2489 (1990); D. Barkley, Physica D **49**, 61 (1991); Phys. Rev. Lett. **68**, 2090 (1992); **72**, 164 (1994).
[32] Q. Ouyang, H. L. Swinney, and G. Li, Phys. Rev. Lett. **84**, 1047 (2000).
[33] K. R. Sreenivasan, Annu. Rev. Fluid Mech. **23**, 539 (1991).
[34] Z.-S. She and L. Liu, Acta Mech. Sin. **19**, 453 (2003); L. Liu and Z.-S. She, Fluid Dyn. Res. **33**, 261 (2003).